Journal of Computer Science

Research Article

Brain Tumor Segmentation and Classification Using HardNet Transformer With Gated Recurrent Unit Model

Saida D[1], Srinivas Adepu[1], Thade Lakshmi Devi[2], Nenavath Chander[3] and Madhu Bhukya[4]

[1]*Department of Computer Science and Engineering, Siddhartha Institute of Engineering & Technology, Ibrahimpatnam, Telangana, India*
[2]*Department of Computer Science and Engineering (Data Science), Avanthi Institute of Engineering & Technology, Hayathnagar, Telangana, India*
[3]*Department of Cybersecurity, Malla Reddy University, Hyderabad, Telangana, India*
[4]*Department of CSE, Malla Reddy (MR) Deemed to be University, Hyderabad, Telangana, 500100, India*

Article history
Received: 13-12-2025
Revised: 21-04-2026
Accepted: 07-08-2026

Corresponding Author:
Saida D
Department of Computer Science and Engineering, Siddhartha Institute of Engineering & Technology, Ibrahimpatnam, Telangana, India
Email: saidan.dhana@gmail.com

Abstract: The uncontrolled growth of brain tumor cells presents a severe health risk, making early diagnosis and accurate classification essential for improving treatment outcomes. However, the existing approaches used for segmentation fail to delineate the tumor regions accurately due to a lack of global contextual information of brain tumors, resulting in poor classification performance. To overcome this limitation, this research proposes a HardNet Transformer based segmentation and Gated Recurrent Unit (HT-GRU)-based classification model for efficient brain tumor classification. Initially, the Magnetic Resonance Images (MRI) are acquired from datasets such as Figshare, BraTS 2020, and Kaggle. Brain tumor features have complex relationships among texture, shape, and intensity features from preprocessed MRI images; therefore, a MobileNet-V2 model is utilized to capture these nonlinear relationships effectively. This approach is beneficial for brain tumor classification, where subtle variations in MRI images, such as tumor texture or boundary features, are crucial for accurate classification. Experimental results of the HT-GRU classification model achieve accuracies of 98.97 and 99.16% for the Figshare and Kaggle datasets, respectively, which are greater than those of previous approaches, such as Binomial Thresholding and Bidirectional Long Short-Term Memory (BT-Bi-LSTM).

Keywords: Brain Tumor, HardNet-Transformer, Gated Recurrent Unit, Magnetic Resonance Images, MobileNet-V2

Introduction

A brain tumor is an abnormal growth of cells in the brain, categorized as either a primary or secondary tumor. Brain tumors are categorized into two types: Primary, when they originate in the brain, and secondary, when they arise from cancer spreading from other organs (Amin et al., 2025). Brain tumors are classified and distinguished according to their dimensions, morphology, and position within the brain. Based on these factors, the tumors are categorized into two types, namely benign and malignant, which are further subclassified into the three most common types: Gliomas, pituitary adenomas, and meningiomas (Ali et al., 2025; Başarslan, 2025; Huang et al., 2025). Magnetic Resonance Imaging (MRI) is a multimodal imaging technology used extensively because of its ability to differentiate between tissues and brain structures based on contrast levels, which helps to detect tumors (Kanchanamala et al., 2025; Amoury et al., 2025). The severity of brain tumors leads to mortality risk; therefore, accurate detection and classification of tumors is critical at early stages for the right diagnosis. In existing research, Machine Learning (ML) and Deep Learning (DL) approaches are extensively utilized for the detection and classification of brain tumors (Hosny et al., 2025; Asiri et al., 2024). However, classification of tumor types from brain MRI images is challenging due to issues such as noise, various resolutions, contrast, and complex brain structures.

Recently, the Convolutional Neural Network (CNN), which is one of the DL approaches, is broadly utilized due to its achievement of better results in various fields, specifically in medical image analysis tasks. The CNN and its variants have the capability to capture most of the

informative features automatically from lower-dimensional images (Nassar et al., 2024). Brain tumor classification based on an artificial intelligence model involves several stages, such as data acquisition, preprocessing, segmentation, feature extraction, and classifying the tumors according to their labels (Shamshad et al., 2024). Nowadays, an automatic brain tumor segmentation model is utilized, where the precise boundary detection of tumors significantly influences the classification model performance. For tumor segmentation from MRI, DL-based segmentation methods are extensively used and show better performance (Zhu et al., 2024). U-shaped Network (U-Net) and Volumetric Network (V-Net) are CNN-based segmentation methods that are employed in existing brain tumor segmentation tasks and help to extract local features in two-dimensional and three-dimensional spaces. Since these conventional segmentation models are limited by the receptive field of convolutions, it makes it difficult to capture global features that are crucial for categorizing the tumor levels (Zhu et al., 2023).

Problem Statement and Objective

Significant variations in shape, texture, size, and tumor location lead to major challenges for accurate tumor segmentation (Popat and Patel, 2026). Hence, the existing brain tumor analysis methods struggle to accurately segment tumor regions and boundaries, which greatly impacts classification performance (Kurdi et al., 2023; Khan et al., 2023). To address the above-mentioned limitations, a HardNet Transformer-based Gated Recurrent Unit (HT-GRU) model is proposed for accurate segmentation and classification of brain tumors from MRI data.

Contributions of Proposed Methodology

The main contributions of this research are as described below:

- The integration of dense connectivity from the HardNet with the vision transformer model ensures accurate tumor boundary delineation and enhances brain tumor classification by learning the global contextual information about tumors
- MobileNet-V2 is utilized to capture discriminative features efficiently from segmented images to enhance the classification of brain tumors
- The GRU-based classification model captures spatial-temporal dependencies from the extracted deep features, leading to improved robustness and reliability in tumor-type classification

Literature Review

To segment and classify brain tumors, various DL approaches are utilized to identify and categorize the tumor types using benchmark datasets. The advantages and limitations of existing brain tumor analysis models are discussed in this section.

Shreeharsha (2024) designed a Binomial Thresholding and Bidirectional Long Short-Term Memory (BT-Bi-LSTM) model to segment and classify brain tumors using MRI. For handcrafted features, Gray-Level Co-occurrence Matrix (GLCM) and Local Ternary Pattern (LTP) techniques were utilized to capture the most relevant features. Dutta et al. (2024) developed a multiclass brain tumor classification model based on an Attention-guided Residual Multiscale convolutional neural Network (ARM-Net) to capture spatial features of tumors from the MRI images. Geetha et al. (2024) explored a hybrid optimization algorithm, namely Sine Cosine Archimedes Optimization (SCAO), to fine-tune the hyperparameters of the DenseNet model. A Segmented Neural Network (SegNet) model was also used to efficiently segment brain tumor regions from MRI images for the extraction of low-level and morphological features.

Sachdeva et al. (2024) presented various Deep CNN (DCNN) methods for brain tumor classification on MRI. Pre-trained models such as Inception-V3, DenseNet-121, EfficientNet B0, MobileNet V3 large, and EfficientNet V2L were utilized for the classification of tumor types. A Global Average Pooling (GAP) layer and a dropout layer were integrated into the pre-trained models to reduce overfitting issues and increase the overall efficiency of the models. Khan et al. (2025) proposed a Manta Ray Foraging Optimization (MRFO) based DenseNet-169 model to fine-tune the hyperparameters of the model for enhancing the classification performance. Additionally, a residual block was incorporated in the optimized DenseNet-169 model to significantly improve feature learning and classify the different types of tumors. Alwadee et al. (2025) designed a Lightweight Three-Dimensional (3D) Attention U-Net with Parallel Convolution Network (LATUP-Net) for segmentation and detection of brain tumors. The designed LATUP-Net was utilized to segment tumor regions accurately with reduced computational cost. Additionally, the integration of parallel convolutions enhanced the feature representation by capturing multi-scale information.

Pourmahboubi et al. (2025) presented a Visual Geometry Group 19 (VGG-19)-based U-Net architecture to extract detailed tumor characteristics for accurate segmentation results. Kusuma and Reddy (2025)

introduced a modified SegNet model and hybrid DL approaches with enhanced texture features to improve segmentation and classification of brain tumors using MRI. The modified SegNet incorporates encoder-decoder symmetry with improved max-pooling that helps in precise edge reconstruction and preservation of fine spatial details of tumor boundaries. Ahsan et al. (2024) explored a DL-based brain tumor detection and segmentation model on MRI data. To segment the tumor region, a 2-Dimensional U-Net (2D-U-Net) was utilized with You Only Look Once (YOLO), Faster Region-based CNN (Faster R-CNN), and Single Shot Detector (SSD) based detection models. The 2D U-Net was employed for pixel-wise segmentation, which helps in accurate brain tumor detection. Moreover, the YOLO-based CNN model effectively recognizes a tumor and reduces false negatives.

For brain tumor analysis, Nancy and Maheshwari (2024) proposed a CNN model utilizing transfer learning and model-agnostic interpretation to enhance both segmentation and classification accuracy. A VGG-19 model with an Attribute Aware Attention (AWA) technique was integrated to segment the brain tumor from MRI data. The VGG-19-based transfer learning model enabled the segmentation network to leverage low-level spatial and texture features that improved boundary detection and segmentation precision.

From the literature review, it is observed that the existing brain tumor analysis models face several limitations, which are summarized as follows: Presence of noise and other artifacts; variation in pixel intensities; different tumor sizes, shapes, and textures; and the tumor region overlapping with brain texture, which makes it difficult for the model to capture significant information. These limitations greatly impact classification performance, which leads to misclassification. To address these limitations, an HT-GRU model is proposed to enhance brain tumor classification using MRI. Conventional CNN-based methods fail to capture global contextual relationships, leading to inaccurate tumor boundary segmentation; this is addressed using the transformer, which enhances global feature learning. Additionally, prior approaches often treat segmentation and classification separately, resulting in suboptimal feature utilization; the proposed unified pipeline ensures better feature flow and improved diagnostic performance. Finally, traditional classifiers such as LSTM introduce higher complexity and slower convergence, which is overcome by using GRU for efficient and faster learning.

Recent developments in deep learning have significantly advanced biomedical image analysis and healthcare systems. Several studies have demonstrated the effectiveness of CNNs, attention mechanisms, and lightweight architectures in improving diagnostic accuracy while maintaining computational efficiency. For instance, a DL-based model developed by Selvan et al. (2025) highlights the integration of sensor-fused IoT data with deep learning models for accurate and efficient health classification. These advancements justify the architectural choices in the proposed work, including the use of attention-based segmentation, lightweight feature extraction, and sequence modeling for classification, aligning the framework with current trends in intelligent healthcare systems.

Methods

The proposed HT-GRU framework follows a structured pipeline consisting of dataset acquisition, preprocessing, segmentation, feature extraction, and classification stages to ensure methodological clarity and consistency. A block diagram for the proposed brain tumor segmentation and classification is presented in Fig. 1. Initially, MRI images acquired from benchmark datasets are preprocessed using resizing, contrast enhancement, and Gaussian filtering techniques to standardize image quality and resolution. Subsequently, the HT model segments the tumor regions by integrating convolutional feature extraction with multi-head self-attention. This architecture effectively captures local spatial details alongside global contextual dependencies to ensure high-precision boundaries. These segmented tumor regions are then fed into the MobileNet-V2 model for deep feature extraction, where a compact yet discriminative 1280-dimensional feature vector is obtained. Finally, these extracted features are fed into a GRU-based classifier, which efficiently learns the inter-feature dependencies and performs accurate tumor classification.

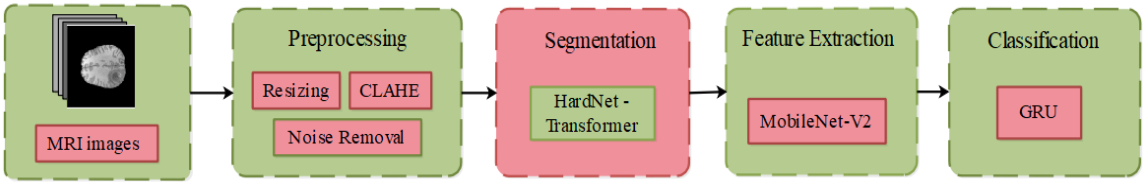

Fig. 1: Proposed brain tumor analysis framework based on the HT-GRU model

Each component in the proposed HT-GRU framework is specifically designed to address limitations observed in existing methods while improving overall performance. The proposed HT model is utilized in the segmentation phase to overcome the limitation of conventional CNNs in capturing global contextual information, which results in more precise tumor boundary delineation (Sobha et al., 2024). MobileNet-V2 is employed in the feature extraction phase to address the high computational complexity of deep networks, providing lightweight and discriminative feature representations that enhance classification efficiency. The GRU classifier is used in the classification phase to overcome the limitations of LSTM, such as higher parameter counts and slower convergence, enabling efficient modeling of feature dependencies with faster training. Together, these components reduce redundancy, improve segmentation accuracy, and enhance classification reliability in brain tumor analysis.

Dataset Acquisition

In this research, three benchmark datasets, BraTS, 2020, Figshare, and the Kaggle MRI dataset, are utilized for brain tumor classification.

BraTs-2020 Dataset

The Brain Tumor Segmentation (BraTS, 2020) dataset is a publicly available repository comprising 369 multi-modal MRI volumes categorized into High-Grade Glioma (HGG - 293) and Low-Grade Glioma (LGG- 76). Each case includes four distinct imaging modalities: T1, T1CE, T2-weighted, and FLAIR, as illustrated in Figure 2.

Figshare Dataset

The Figshare dataset is a publicly available dataset (Figshare, 2017) and is categorized into a multi-class dataset that comprises various tumor classes. Fig. 3 illustrates some of the MRI data from the Figshare dataset. These data are divided based on the different perspectives of sagittal, coronal, and axial. The Figshare dataset contains 930 samples obtained from 62 patients with pituitary tumors, 1426 samples from 89 patients who suffered from glioma tumors, and 708 samples from 82 patients who were diagnosed with meningioma tumors.

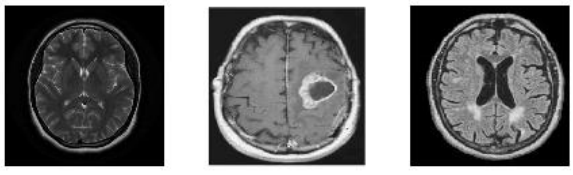

Fig. 2: Sample images of the BraTS, 2020 dataset for brain tumor segmentation

Kaggle Dataset

The Kaggle dataset is an open-access dataset Masoud (2021), which consists of 3264 brain images that are sub-categorized into 926 glioma, 937 meningioma, and 901 pituitary tumor classes. Fig. 4 presents input MRI data used for training and validation of the proposed brain tumor analysis model. These data are fed as inputs to the preprocessing phase.

The data obtained from benchmark datasets are divided into training and testing sets using a patient-wise splitting strategy, ensuring that the MRI images from the same patient are not distributed across multiple subsets. This prevents the proposed model from overlapping patient data between training and testing phases.

The proposed framework is designed to handle both segmentation and classification tasks across heterogeneous datasets according to dataset-specific objectives. For the BraTS dataset, the model performs fine-grained segmentation of tumor sub-regions: The Tumor Core (TC), Whole Tumor (WT), and Enhancing Tumor (ET). In contrast, for the Kaggle and Figshare datasets, the proposed segmentation model serves as a preprocessing step to isolate the region of interest and enhance classification accuracy for gliomas, meningiomas, and pituitary tumors. This unified and adaptable design ensures that the proposed segmentation enhances feature localization, while classification is performed based on dataset-specific labels, which maintains consistency without combining the two distinct tasks, namely segmentation and classification.

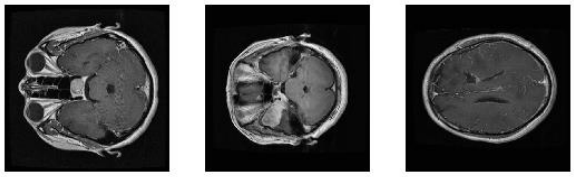

Fig. 3: MRI images of the Figshare dataset utilized for brain tumor classification

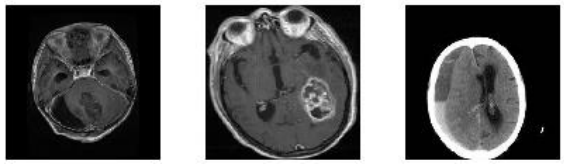

Fig. 4: Sample input images of the Kaggle brain tumor dataset used for brain tumor analysis

Preprocessing

The acquired brain images are fed as input for the preprocessing phase to enhance the images into a suitable form for further classification. The MRI images in the dataset have varying dimensions and contain noise introduced during the acquisition

process, which leads to poor performance in brain tumor classification. For preprocessing, resizing and Gaussian filters are used to reduce the dimensions and remove noise from the brain images:

- Resizing: Since the input images acquired from three different datasets have various resolutions, this affects the model training and degrades the classification accuracy. Therefore, the resizing technique transforms all the acquired brain MRI images into uniform resolutions to avoid poor segmentation and enhance model performance. The input MRI images are resized from $240 \times 240 \times 155$ to224×224
- Contrast-Limited Adaptive Histogram Equalization (CLAHE): This method enhances image clarity by redistributing pixel intensity and boosting contrast, making it ideal for identifying subtle features in medical imaging. The clip limit enhances the performance of the CLAHE technique and the histograms of each nonoverlapping region that converge to a level below this parameter. This CLAHE helps to enhance the tumor boundaries, which improves segmentation. The clip limit β form is mathematically represented in Eq. (1):

$$\beta = \frac{MN}{G}\left\{1 + \frac{\alpha}{100}(AS_{max} - 1)\right\} \quad (1)$$

Where α denotes the clip factor; AS_{max} indicates the maximum allowance slope; G indicates the number of grayscale levels. M and N denote the number of pixels in each region; these contrast-enhanced images are passed to the noise removal filter:

- Noise Removal: The contrast-enhanced images are then smoothed by a Gaussian filter, which mitigates random noise and preserves edges as well as the important information during training. The Gaussian filter improves brain images by filtering out unnecessary noise, which helps to focus more on features with meaningful information. The mathematical expression of a Gaussian kernel with a radial basis function is given by Eq. (2):

$$G(x,y) = \frac{1}{2\pi\sigma^2}\, e^{-\frac{x^2+y^2}{2\sigma^2}} \quad (2)$$

Where x and y indicate the locations of image pixels, $G(x,y)$ represents the Gaussian kernel function, and σ indicates the standard deviation.

The 3D MRI volumes from the BraTS dataset are processed using a slice-wise 2D approach to balance computational efficiency and model complexity. Each 3D volume is decomposed into axial slices, which are then individually processed by the proposed framework. This approach significantly reduces memory requirements and enables the use of pretrained 2D convolutional architectures such as MobileNet-V2. To maintain data integrity and prevent leakage, patient-wise splitting is employed to ensure that all slices from a single patient are assigned exclusively to either the training or testing subset. While 3D models capture volumetric context, a 2D approach offers a practical balance between computational efficiency and competitive accuracy.

Segmentation

After preprocessing, the denoised MRI images are then passed to the proposed HardNet approach, which is an enhanced version of the DenseNet structure. HardNet reduces the total number of model parameters and speeds up the network operations using a sparse connection strategy. Fig. 5 represents the architecture of the proposed HT-based segmentation model employed for brain tumor analysis. Specifically, layer k is only connected to previous layers, where $k - 2^1 - 2^{nk} - 2n$ is a valid integer (i.e., n ≥ 0, k−2 n ≥ 0). This design allows intermediate layers (e.g., layers 1 to 2^{n-1}) to be cleared from memory after use, thereby reducing memory usage and computation.

The input consisted of a batch of n images represented as $x \in RH \times W \times C \times n$:

- Where H and W are the height and width of the preprocessed image
- C: number of image channels
- n: number of input images

The HardNet-based CNN extracts the features by downsampling the input images and transforming them into a lower-resolution representation $x \in R\,H\,16 \times W\,16 \times C \times$ n. This coarse feature extraction helps capture the essential spatial patterns while reducing the computational load. The extracted low-resolution features are then passed to the upsampling layers for further processing in the segmentation network.

In this research, Multi-Head Attention (MHA) is utilized instead of the self-attention mechanism in the Vision Transformer (ViT) (Chaoyang et al., 2024), which processes the input image by transforming it into three matrices: Query (Q), key (K), and value (V). Fig. 6 represents the architecture of the vision transformer block.

A similarity matrix (QK^T) is computed by taking the product of the query and transposed key matrices, with the resulting magnitudes representing the degree of correlation between features. This matrix is then subsequently normalized using the softmax function to

produce final attention weights. These weights are then used to scale the value matrix ( )V, which permits the model to concentrate on the significant set of features. The mathematical formulation of the MHA used in the HarDNet model is given by the following Eqs. (3, 5):

$$Attention(Q,K,V) = Softmax\left(\frac{QK^T}{\sqrt{d_k}}\right)V \quad (3)$$

$$head_i = Attention\left(QW_i^Q,\ KW_i^K, VW_i^V\right) \quad (4)$$

$$Multi(Q,K,V) = Concat(head_i, \ldots, head_h)W^o \quad (5)$$

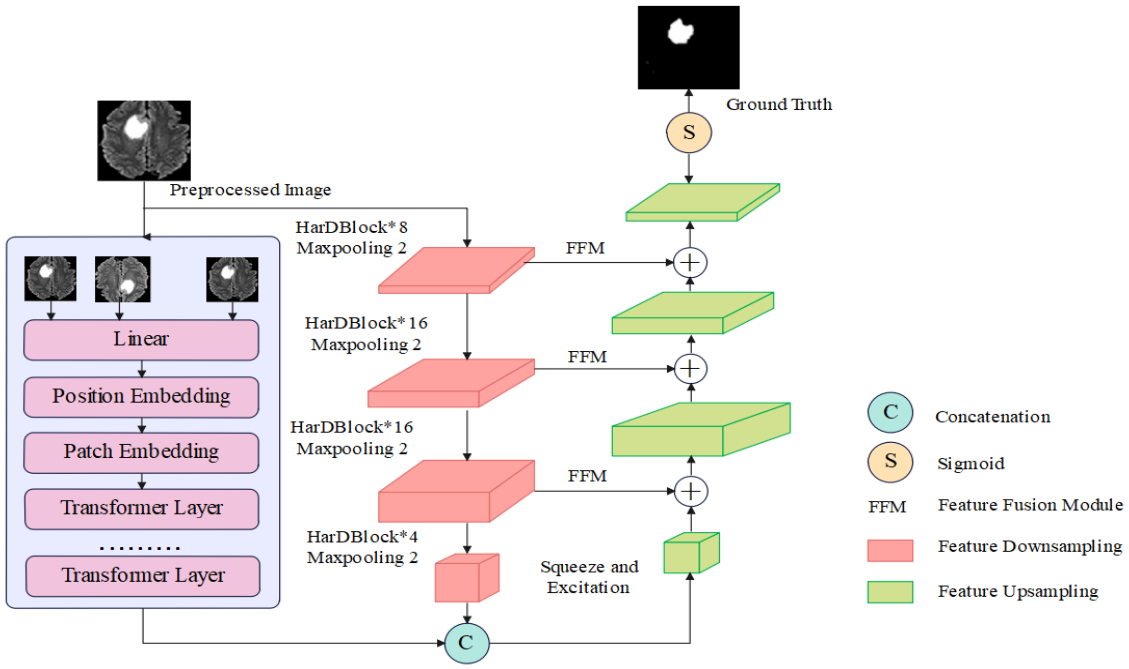

Fig. 5: Architecture of the proposed HT-based segmentation model

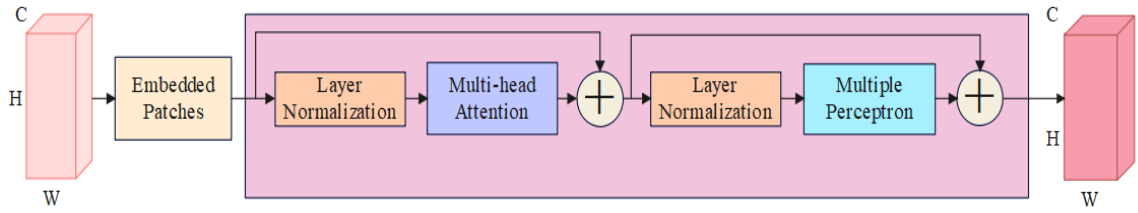

Fig. 6: Vision Transformer block

The HardNet module extracts local feature information from the input image through multiple convolutional layers. These features are then utilized to generate an attention map by computing the product of the resulting weight and value matrices. Meanwhile, a transformer module divides the image into patches and captures the global feature information. Both global and local features are then integrated through a summation operation, thereby enabling the segmentation network to learn multi-dimensional representations from the preprocessed image. This fused feature information is then passed to the decoder by the Squeeze and Excitation (SE), which enhances the important feature channels while suppressing irrelevant ones. Since the brain tumors vary in shape, size, texture, and intensity across patients and MRI modalities (T1, T2, FLAIR), this greatly impacts classification results. Existing segmentation methods, such as SegNet, failed to capture this varying information precisely due to weak boundary delineation. However, the proposed HT model captures the contextual information, which helps to recognize the varying tumor regions. Also, this information leads to accurate boundary delineation based on their relationship to surrounding tissues rather than just intensity values. The segmented images are passed to the feature extraction phase. Fig. 7. (a) and (b) present sample segmented output images by the HT model.

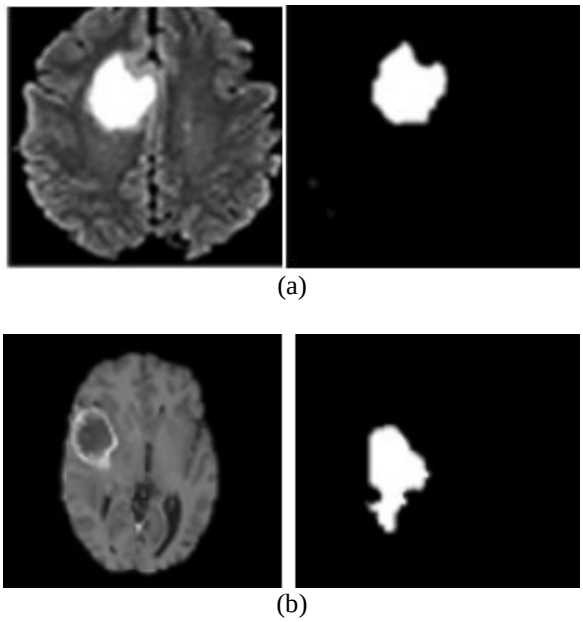

Fig. 7: (a) and (b) sample segmented output images using the HT model

Feature Extraction

After segmentation, the segmented images are fed into the input layer of the MobileNet-V2 model (Islam et al., 2023) for extracting deep features, which helps to classify the types of tumors efficiently. Though the proposed HT model captures both rich spatial and contextual representations during segmentation, its primary objective is accurate pixel-level localization rather than compact feature representation for classification. Therefore, a MobileNet-V2 approach is incorporated as a dedicated feature extractor to capture lightweight and discriminative feature embeddings, which are most suitable for precise classification. Additionally, the MobileNet-V2 approach employs depthwise separable convolutions and inverted residual structures to produce efficient and low-dimensional feature vectors, which reduce computational complexity while preserving critical information.

The MobileNet-V2-based feature extractor model involves convolutional operations followed by batch normalization and an activation function, and finally, strided max pooling is applied to the normalized vector. Similarly, the remaining layers follow a similar structure, and for training, a stochastic gradient descent algorithm is utilized in the MobileNet-V2 feature extractor model. This architecture of MobileNet-V2 efficiently extracts both low- and high-level features of tumors at various scales from the preprocessed images. The lower layers in MobileNet-V2 extract features such as shapes, textures, and edges, whereas the deeper layers extract abstract and complex features. The MobileNet-V2-based feature extraction model extracts a 1280-dimensional feature vector from the final convolutional or global average pooling layer. These features include tumor boundary, surface texture, brightness variations, and structural composition. Such rich representations aid in the accurate classification of tumor types and grades.

Classification

After feature extraction, the extracted features are fed into a GRU, which is a type of LSTM model that allows learning tumor patterns efficiently. By capturing the temporal dependencies and tumor patterns across the feature sequence, the GRU model produces a hidden state representation that summarizes the tumor characteristics. A final fully connected layer maps these features to their corresponding labels, for identifying the tumor as a glioma, meningioma, or pituitary tumor. Furthermore, the GRU model processes the features in sequence order, which is more stable when compared with models that process each feature individually. The proposed GRU model architecture involves two gates: The reset gate, which controls how much of the past information is forgotten, and the update gate, which selects the memory information that continues to be retained until the current moment. Fig. 8 illustrates the GRU architecture utilized for the categorization of brain tumors.

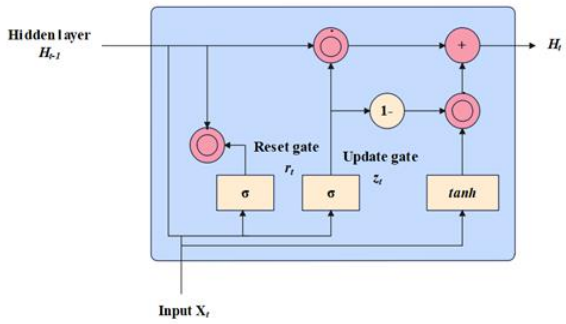

Fig. 8: GRU architecture utilized for brain tumor classification

These two gates determine the last transmitted hidden state h_{t-1} and input x_t of the current node, which is mathematically formulated in Eqs. (6) and (7):

$$z_t = Sigmoid\ (W_{xz}x^t + W_{hz}h^{t-1} + b_z) \quad (6)$$

$$r_t = Sigmoid\ (W_{xr}x^t + W_{hr}h^{t-1} + b_r) \quad (7)$$

Here, x^t is the input, z_t and r_t are the update and reset gates, and h^{t-1} is the previous hidden state. The weights and biases for these gates are denoted by W (W_{xz}, W_{xr}) and b (b_r, b_z) respectively, with Sigmoid as the activation function. In a GRU, these two gates manage the information flow by determining which features to retain or discard, effectively addressing the vanishing gradient issue.

To fine-tune the hyperparameters of the GRU model, a stochastic gradient descent algorithm integrated with the Cross Entropy (CE) loss function is employed in this research to train the model. Subsequently, these output class labels are converted into probabilistic outcomes using a softmax function, which is commonly utilized for multiclass classification. In this research, a categorical CE loss function is used to obtain probabilistic outputs of the detected categories by the GRU model, which is represented mathematically in Eq. (8):

$$L_{CE} = -Y_n^T . logZ_n = -\sum_i^c y_{i,n} log(z_{i,n}) \quad (8)$$

The CE loss function L_{CE} quantifies the discrepancy between the predicted probability vector Z_n and the one-hot encoded ground truth Y_n, guiding the model to minimize pixel-wise misclassification. In segmentation, this ensures the precise delineation of complex tumor boundaries, while in classification, it refines the model's ability to differentiate between distinct tumor pathologies. The comprehensive integration of these components, including the feature extraction and gating mechanisms, is detailed in Algorithm 1, which outlines the HT-GRU model's end-to-end pipeline for robust brain tumor analysis.

Algorithm 1

Start
Input: Images from BraTS, 2020, Figshare, and Kaggle datasets
Output: Segmented image and output class
Procedure:
Preprocessing
For $m = 1$ to j do
Read and resize the image I.
Remove noise using a Gaussian filter
End for
Segmentation by HT
For each preprocessed MRI image, do
Extract local feature maps using HardNet convolution blocks.
Divide the image into patches and compute Q, K, V matrices.
Apply MHA to capture the global context.
Employ SE to enhance informative channels.
Decode fused features through upsampling layers.
Generate a tumor segmentation mask.
End For
Feature Extraction
For each segmented tumor image, do
Feed the segmented region to MobileNet-V2.
Obtain the final 1280-dimensional feature vector.
Store the extracted feature vector.
End For
Classification
Initialize GRU with update and reset gates.
For each feature vector, do
Feed the feature sequence into the GRU layer.
Compute r_t and z_t.
Generate a h_t capturing temporal dependencies.
Pass the final hidden state through a fully connected layer.
Apply Softmax to obtain a probability score for each tumor class.
End For
End

The integration of HardNet and MobileNet-V2 provides a lightweight architecture that ensures faster inference with reduced computational complexity. HardNet enhances the tumor segmentation accuracy through efficient dense connectivity, whereas MobileNet-V2 extracts high-quality features with minimal parameters. The GRU classifier captures temporal dependencies among features, thereby improving the classification robustness.

Results and Discussion

Experimental results of the HT-GRU model, which is employed for brain tumor analysis from MRI data using the BraTs-2020, Figshare, and Kaggle datasets, are depicted in this section. The proposed HT-GRU method is implemented using the MATLAB (R2020b) software tool with a Windows 10 OS system configuration, an Intel i5 processor, and 16 GB RAM. The hyperparameter settings of the HardNet and GRU models used for segmentation and classification are depicted in Table 1. For hyperparameter tuning of these models, a stochastic gradient descent optimizer is utilized to improve classification performance.

Table 1: Hyperparameter settings of the proposed HT-GRU model

Parameters	Value
HT based segmentation	
Input image size	224×224×3
Convolutional kernel size	3×3
Activation function	ReLU
Patch size (in ViT)	16×16
Dropout	0.1
Learning rate	0.0001
Segmentation loss	Binary cross-entropy loss function
GRU	
Input feature dimension	1280 D
te activations	Sigmoid
Hidden state activation	Tanh
Dropout	0.2
Output activation	Softmax
Learning rate	0.001
Loss function	Categorical cross-entropy loss function
Batch size	32

To ensure reproducibility and avoid experimental bias, a well-defined experiment protocol is followed during model training and evaluation. In this research, the acquired MRI data from benchmark datasets are divided into training and testing sets using a patient-wise splitting strategy, which ensures that the MRI images from the same patient are not distributed across multiple subsets. This data split prevents overlap of patient data between training and testing phases. This strategy ensures that the model evaluation reflects true generalization performance rather than random memorization. Moreover, the preprocessing steps, including resizing, contrast enhancement, and noise filtering, are performed uniformly only on the training set. Additionally, k-fold cross-validation is performed to validate the robustness and generalization capability of the proposed framework.

Evaluation Metrics

To evaluate the effectiveness of the HT-GRU model, a comprehensive set of performance metrics is employed across both the segmentation and classification tasks. Evaluation metrics such as precision, accuracy, specificity, sensitivity, the Dice coefficient, and Hausdorff Distance (HD) are considered for evaluation, which are expressed mathematically in Eqs. (9) (15):

$$Accuracy = \frac{TP+FN}{TP+TN+FP+FN} \times 100 \quad (9)$$

$$Precision = \frac{TP}{TP+FP} \times 100 \quad (10)$$

$$Sensitivity = \frac{TP}{/(TP+F} \quad (11)$$

$$Specificity = \frac{TN}{/(TN+FP} \quad (12)$$

$$F1 - Score = 2 \times \frac{Precision \times Recall}{Precision+Recall} \quad (13)$$

$$DSC = \frac{2TP}{2TP+FP+FN} \quad (14)$$

$$HD(T,P) = max\begin{pmatrix} sup\ inf\ d\ (t,p) & sup\ inf\ d\ (t,p) \\ t \in T \quad p \in P' & p \in P \quad t \in T \end{pmatrix} \quad (15)$$

Where True Positive, True Negative are denoted as TP, TN; False Positive, False Negative are represented as FP, FN; T stands for actual or ground-truth region, For surface-based metrics, T and P denote the ground-truth and predicted lesion regions, where $d\ (t,p)$ measures the distance between points on these
between points on these surfaces. The operators inf and sup denote the infimum and supremum and are utilized to define the boundaries of these distance calculations.

Quantitative and Qualitative Analysis

To assess the proposed HT-GRU model, this section details experimental results using the BraTS, 2020, Figshare, and Kaggle datasets. The efficacy of the proposed segmentation and classification methods is rigorously compared with existing state-of-the-art architectures.

Segmentation

Table 2 represents the evaluation of the proposed HT-based segmentation method for brain tumor segmentation. For evaluation, existing DL models, such as U-Net, V-Net, CNN (encoder and decoder), and DeepLabV3, are considered alongside the proposed HT-based segmentation model. The presented segmentation method attained an accuracy of 98.46%, which is higher than that of the existing DL-based classifier methods.

Feature Extraction

Various pre-trained models, such as baseline CNN, DenseNet-169, EfficientNet-B7, and ResNet-50, are considered for the performance evaluation with the MobileNet-V2 model in brain tumor classification. Figs. 9-11 depict the performance analysis of the MobileNet-V2-based feature extraction method using the Figshare, Kaggle, and BraTS, 2020 datasets, respectively.

Table 2: Performance of the proposed HT-based segmentation model using the BraTs-2020, Figshare, and Kaggle datasets

Datasets	Methods	Performance Matrices		
		Accuracy (%)	Dice Similarity Coefficient (%)	Hausdorff distance (%)
Figshare	U-Net	95.82	95.22	94.85
	V-Net	95.46	92.57	94.99
	CNN (encoder and decoder)	97.59	96.98	97.20
	DeepLab-V3	96.57	95.37	94.57
	Proposed HardNet	98.97	97.76	97.53
Kaggle	U-Net	97.70	97.47	97.15
	V-Net	95.31	95.23	94.98
	CNN (encoder and decoder)	93.22	93.08	92.88
	DeepLab-V3	98.84	99.04	99.87
	Proposed HardNet	99.16	98.97	98.95
BraTs, 2020	U-Net	95.82	95.22	94.85
	V-Net	89.74	86.46	87.46
	CNN (encoder and decoder)	79.35	78.46	78.44
	DeepLab-V3	95.46	92.57	94.99
	Proposed HardNet	99.92	98.85	98.80

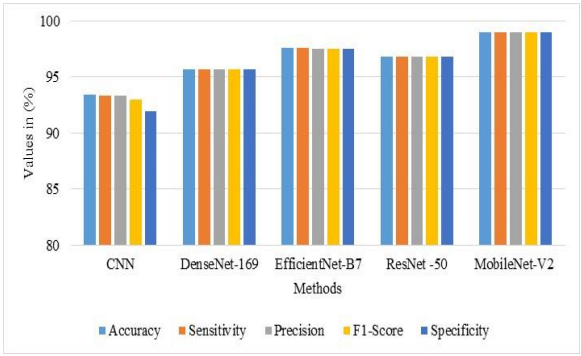

Fig. 9: Performance evaluation of the feature extraction method using the Figshare dataset for brain tumor analysis

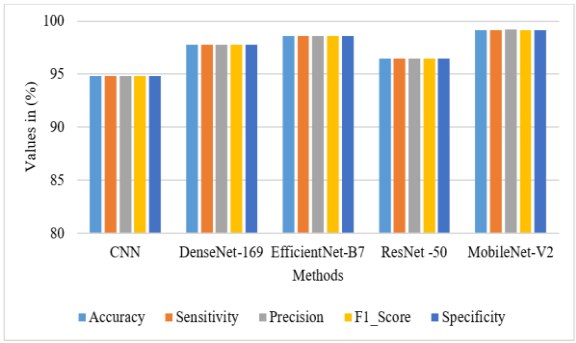

Fig. 10: Performance comparison of MobileNetV2-based feature extraction with pre-trained models on the Kaggle brain tumor dataset

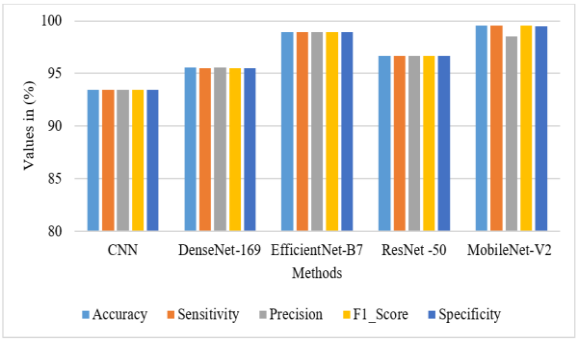

Fig. 11: Performance evaluation of MobileNet-V2 in brain tumor classification using the BraTS, 2020 dataset

From the above results, the MobileNet-V2 model, which is utilized for feature extraction in this research, outperforms the other pre-trained models.

In contrast, the traditional CNN model and ResNet-50 face difficulties in capturing fine-grained tumor details, while DenseNet-169 is a deeper architecture that leads to an increase in computational complexity.

Though the EfficientNet-B7 model is powerful, it is prone to overfitting issues on limited medical data, which negatively affects the classification results.

Classification

In this quantitative and qualitative analysis of the proposed HT-GRU model, several DL classifiers, such as baseline CNN, Recurrent Neural Network (RNN), LSTM, and GRU models, are utilized for the performance evaluation with the proposed model in brain tumor classification. Tables 3-5 summarize the performance analysis of the HT-GRU-based classification model in terms of with and without segmentation using Figshare, Kaggle, and BraTS, 2020 datasets, respectively.

The above results demonstrate that the HT-GRU method achieves superior results in brain tumor segmentation and classification. The HT model captured fine-grained tumor structures efficiently, while the transformer module models long-range dependencies to preserve global context.

Table 6 represents cross-validation of the proposed HT-GRU-based classification model in terms of various k-folds for three distinct datasets. Cross-validation is done to validate the performance of various DL-based classifiers in brain tumor classification by splitting the data into various k-folds. These results confirmed that the proposed HT-GRU model achieves superior results in k = 5 folds due to an optimal balance between training and validation data. These results ensure that the proposed model reduces both underfitting and overfitting issues while maintaining stable performance across all three datasets.

Table 3: Performance evaluation of the HT-GRU model in brain tumor classification using the Figshare dataset

Segmentation	Methods	Accuracy (%)	Sensitivity (%)	Precision (%)	F1-Score (%)	Specificity (%)
No	CNN	90.63	90.60	90.61	90.61	90.62
	RNN	93.70	93.68	93.69	93.67	93.66
	LSTM	96.34	96.33	96.32	96.31	96.30
	GRU	97.24	97.21	97.23	97.20	97.22
Yes	HT-CNN	94.44	94.42	94.43	94.42	94.43
	HT-RNN	95.97	95.96	95.98	95.94	95.95
	HT-LSTM	97.56	97.54	97.55	97.52	97.53
	Proposed Method HT-GRU	98.97	98.96	98.98	98.975	98.95

Table 4: Quantitative evaluation of the proposed HT-GRU model versus existing DL architectures for brain tumor classification using the Kaggle dataset

Segmentation	Methods	Accuracy (%)	Sensitivity (%)	Precision (%)	F1-Score (%)	Specificity (%)
No	CNN	91.57	91.55	91.56	91.55	91.54
	RNN	95.90	95.88	95.89	95.87	95.87
	LSTM	96.71	96.73	96.72	96.72	96.74
	GRU	97.66	97.64	97.65	97.65	97.93
Yes	HT-CNN	92.68	92.66	92.67	92.67	92.63
	HT-RNN	96.54	96.52	96.53	96.51	96.52
	HT-LSTM	98.42	98.41	98.43	98.40	98.42
	Proposed Method HT-GRU	98.86	97.97	98.88	98.87	97.96

Table 5: Evaluation of the HT-GRU model with existing DL approaches on the BraTS, 2020 dataset

Segmentation	Methods	Accuracy (%)	Sensitivity (%)	Precision (%)	F1-Score (%)	Specificity (%)
No	CNN	91.57	91.55	91.56	91.55	91.54
	RNN	95.90	95.88	95.89	95.87	95.87
	LSTM	96.71	96.73	96.72	96.72	96.74
	GRU	97.66	97.64	97.65	97.65	97.93
Yes	HT-CNN	92.68	92.66	92.67	92.67	92.63
	HT-RNN	96.54	96.52	96.53	96.51	96.52
	HT-LSTM	98.42	98.41	98.43	98.40	98.42
	Proposed Method HT-GRU	99.92	99.82	99.86	99.84	98.74

Table 6: Cross-fold validation of the HT-GRU model using the k-fold technique, utilizing three benchmark datasets in brain tumor classification

K-folds	Figshare		Kaggle		BraTs, 2020	
	Accuracy (%)	Precision (%)	Accuracy (%)	Precision (%)	Accuracy (%)	Precision (%)
k = 2	97.86	97.90	98.10	98.15	98.70	98.65
k = 3	98.35	98.40	98.65	98.70	99.10	99.05
k = 5	98.97	98.98	99.16	99.18	99.92	99.86
k = 7	98.75	98.78	98.85	98.87	99.30	99.28
k = 9	98.60	98.65	98.85	98.88	99.20	99.18

Computational Complexity Analysis and Statistical Analysis

Table 7 illustrates the statistical analysis and computational complexity of the HT-GRU model. Statistical analysis is performed to evaluate the effect and significance of the model results based on a hypothesis. In this research, the p-value is the probability of observing the test under the null hypothesis, and confidence intervals are considered for the evaluation of the HT-GRU. The results show that HT-GRU achieves $p = 0.029$ in terms of accuracy, confirming that the model is statistically significantly better than existing models. Additionally, computational complexity analysis is performed to analyze the resources, time (seconds), and memory usage (Gigabytes (GB)) of the HT-GRU model in the classification of brain tumors. The HT-GRU model achieves less computational time and memory usage, which ensures computational efficiency.

Ablation Study

Table 8 represents the ablation study of the proposed HT-GRU-based brain tumor analysis model in terms of different configurations using distinct benchmark datasets. The baseline GRU model exhibits lower accuracy due to the absence of spatial feature extraction and segmentation, and the Dice score is not applicable since no segmentation is performed. The inclusion of preprocessing significantly enhances performance by improving image quality and reducing noise, leading to better feature learning. Further improvement is observed with MobileNet-V2, which provides efficient and discriminative feature extraction. The introduction of the proposed HT model strengthens tumor segmentation capability by capturing complex spatial patterns, which results in higher Dice scores. Finally, the complete proposed brain tumor analysis model achieved the best performance due to the combined effect of precise segmentation, enhanced feature representation, and accurate tumor classification.

Comparative Analysis

A comparative study of the proposed HT-GRU with previous segmentation and classification models using Figshare, Kaggle, and the BraTS, 2020 dataset is presented in this section. Table 9 presents a comparative evaluation of the HT-GRU model using the Figshare

dataset with existing classification methods, such as SegNet and SCAO (Geetha et al., 2024).

Table 10 provides a comparative study of the HT-GRU model using the Kaggle dataset. The proposed HT-GRU method is compared with existing classification methods used in brain tumor classification, such as EfficientNet-B0 (Sachdeva et al., 2024) and MRFO-based DenseNet-169 (Khan et al., 2025).

Table 11 demonstrates a comparative analysis of the HT-GRU model using the BraTS, 2020 dataset. The proposed HT-GRU method is compared with existing classification methods used in brain tumor classification, such as BT-Bi-LSTM (Shreeharsha, 2024), ARM-Net (Dutta et al., 2024), and SegNet SCAO (Geetha et al., 2024).

Research Implications

This comparative analysis highlights the significant implications of the proposed HT-GRU model, which achieves precise segmentation and reliable classification performance with lower computational cost. From these results, the proposed HT-GRU framework proves to be a reliable and efficient brain tumor analysis model on MRI data.

Table 7: Statistical analysis and computational complexity of brain tumor classification

Methods	p-value	Confidence interval (%)	Memory usage (GB)	Computational time (s)
CNN	0.071	0.921-0.943	1.85	112
RNN	0.068	0.927-0.948	2.10	148
LSTM	0.052	0.934-0.956	2.25	132
Proposed HT-GRU	0.029	0.948-0.969	1.65	98

Table 8: Ablation study of an HT-GRU-based brain tumor analysis model using MRI data

Configuration	Figshare			Kaggle			BraTs, 2020		
	Accuracy (%)	Precision (%)	Dice (%)	Accuracy (%)	Precision (%)	Dice (%)	Accuracy (%)	Precision (%)	Dice (%)
GRU	92.15	91.80	N/A	92.88	92.34	N/A	93.20	92.85	N/A
Preprocessing + GRU	95.12	94.85	93.48	95.86	95.42	94.73	96.18	95.90	94.82
Preprocessing + MobileNet V2 + GRU	96.74	96.30	95.12	97.15	96.88	96.05	97.45	97.10	96.20
Preprocessing + proposed HT + GRU	97.82	97.55	96.48	98.05	97.80	97.12	98.20	97.95	97.05
Proposed model (Preprocessing + MobileNet V2 proposed HT + GRU)	98.60	98.65	97.76	98.85	98.88	98.97	99.20	99.18	98.85

Table 9: Comparative evaluation of the HT-GRU with existing classification approaches using the Figshare dataset

Methods	Accuracy (%)	Specificity (%)	Sensitivity (%)	Precision (%)	F1-score (%)
SegNet and SCAO (Geetha et al., 2024)	92.7	92.5	91.4	N/A	N/A
Proposed method HT-GRU	98.97	98.95	98.96	98.98	98.975

Table 10: Comparative study of the HT-GRU with existing classification approaches using the Kaggle dataset

Methods	Accuracy (%)	Specificity (%)	Sensitivity (%)	Precision (%)	F1-score (%)
EfficientNet-B0 (Sachdeva et al., 2024)	96.25	N/A	N/A	N/A	N/A
MRFO-based DenseNet-169 model (Khan et al., 2025)	98.53	N/A	97.8	98.06	N/A
Proposed method HT-GRU	98.86	97.96	97.97	98.88	98.87

Table 11: Comparative study of the HT-GRU with existing classification approaches using the BraTS, 2020 dataset

Methods	Accuracy (%)	Specificity (%)	Sensitivity (%)	Precision (%)	F1-score (%)
BT-Bi-LSTM (Shreeharsha, 2024)	99.89	N/A	99.62	99.76	N/A
ARM-Net (Dutta et al., 2024)	97.11	N/A	97.97	96.66	96.87
SegNet and SCAO (Geetha et al., 2024)	93.0	92.0	92.3	N/A	N/A
Proposed method HT-GRU	99.92	98.74	99.82	99.86	99.84

Discussion

The proposed HT-GRU is used in brain tumor segmentation and classification, and it attains better results in categorizing the tumors precisely. Existing detection approaches have several limitations in disease detection, such as the BT-Bi-LSTM (Shreeharsha, 2024) model, which failed to classify the tumors efficiently due to its sensitivity to noise and intensity variation. The ARM-Net (Dutta et al., 2024) model failed to classify tumors accurately because of variations in tumors that are not properly segmented. The SegNet-based brain tumor segmentation and SCAO model (Geetha et al., 2024) lacks contextual information, affecting segmentation and leading to misclassification. Due to the presence of noise, image quality affects the training of various DCNN methods (Sachdeva et al., 2024), resulting in inaccurate classification results. The MRFO-based DenseNet-169 model (Khan et al., 2025) failed to capture key information about tumor regions, making it difficult to identify and classify the tumor types accurately.

To address these limitations, an HT-GRU model is proposed in this research for accurate brain tumor classification by integrating local and global feature learning. The proposed HT model enhances segmentation accuracy by combining efficient convolutional operations with attention-based contextual modeling that enables precise tumor boundary delineation even in complex MRI scenarios. Additionally, the MobileNet-V2 enables efficient feature extraction with reduced computational complexity, while the GRU classifier captures inter-feature dependencies, leading to accurate classification performance. When compared to conventional CNN-based approaches that rely solely on local receptive fields, the proposed framework leverages global contextual information, which improves its capability to handle variations in tumor size, shape, and intensity. These factors collectively contribute to the superior performance observed across multiple benchmark datasets.

Limitations and Future Work

The proposed HT-GRU model achieves high performance in brain tumor analysis, but it has certain challenges. First, the model depends on labeled MRI datasets, which limit its applicability in scenarios with scarce annotated medical data. Also, in this research, the proposed model is primarily evaluated on MRI data for brain tumor analysis. However, its architecture is modality-independent and is also suitable for Computed Tomography (CT) image-based brain tumor analysis. The advantages of the proposed HT-GRU model provide similar improvements in noise reduction and feature representation, which result in enhanced classification accuracy without performance degradation in CT image-based brain tumor analysis. Second, robustness against noisy inputs and adversarial perturbations is not explicitly evaluated. Future work will focus on addressing these limitations by integrating diverse datasets, real-time validation, and advanced enhancement methods.

Conclusion

The HT-GRU algorithm was proposed for efficient feature selection and brain tumor classification. Brain tumor features had complex relationships between texture, shape, and intensity features in MRI, and therefore, the HT–GRU model was employed to capture these nonlinear relationships effectively. This was beneficial for brain tumor classification, where subtle variations of MRI images, such as tumor texture or boundary features, were crucial for accurate classification. Initially, the brain images were preprocessed to enhance image quality by removing noise from the MRI images. Then, the brain tumors were segmented by the anisotropic diffusion method, and MobileNet-V2 was used to capture features from the segmented images. Next, the most significant factors that helped to enhance brain tumor classification were selected by HT-GRU and classified by the LSTM model. Experimental results of the HT-GRU method attained an accuracy of 99.56%, which was greater than that of existing approaches such as SegNet, SCAO, and EfficientNet-B0. As future work, an improved DL model will be utilized for segmentation and classification to enhance the accurate classification of brain tumor regions.

Table Notation:

Notations	Descriptions
$\boldsymbol{\alpha}$	Clip factor
$\boldsymbol{AS_{max}}$	Maximum allowable slope
$\boldsymbol{G}$	Number of grayscale levels
$\boldsymbol{M}$ and $\boldsymbol{N}$	Number of pixels in each region
$\boldsymbol{x}$ and $\boldsymbol{y}$	Locations of image pixels
$\boldsymbol{G(x,y)}$	Gaussian kernel function
$\boldsymbol{\sigma}$	Standard deviation
$\boldsymbol{H}$ and $\boldsymbol{W}$	Height and width of preprocessed image
$\boldsymbol{C}$	Number of image channels
$\boldsymbol{n}$	Number of input images
$(\boldsymbol{Q})$,$(\boldsymbol{K})$, and $(\boldsymbol{V})$	Query, Key, and Value
$(\boldsymbol{K^T})$	Key matrix
$(\boldsymbol{QK^T})$	Similarity matrix
$\boldsymbol{h_{t-1}}$	Hidden state
$\boldsymbol{x_t}$	Input
$\boldsymbol{z_t}$ and $\boldsymbol{r_t}$	Update and reset gates
$\boldsymbol{W_{xz}}$ and $\boldsymbol{W_{xr}}$	Weights of update and reset gates
$\boldsymbol{b_r}$ and $\boldsymbol{b_z}$	Bias of the reset and update gates
$\boldsymbol{Sigmoid}$	Activation function
$\boldsymbol{L_{CE}}$	Cross-Entropy (CE) loss function
$\boldsymbol{Y_n}$	One-hot encoded ground truth vector
$\boldsymbol{Z_n}$	Predicted probability vector
$\boldsymbol{y_{i,n}}$ and $\boldsymbol{z_{i,n}}$	ith elements of $\boldsymbol{Y_n}$ and $\boldsymbol{Z_n}$

Acknowledgment

The authors express their sincere gratitude to their respective institutions Siddhartha Institute of Engineering & Technology, Avanthi Institute of Engineering & Technology, Malla Reddy University, and TRR College of Technology for providing the necessary support, facilities, and encouragement throughout the preparation of this manuscript.

Funding Information

The authors confirm that this research did not receive any specific grant from funding agencies in the public, commercial, or not-for-profit sectors.

Author's Contributions

Saida D: Conceptualization, methodology design, supervision, manuscript drafting.

Srinivas Adepu: Data collection, analysis, validation, and manuscript refinement.

Thade Lakshmi Devi: Literature review, experimental setup, and result interpretation.

Nenavath Chander: Technical support, data verification, and editing of the manuscript.

Madhu Bhukya: Visualization, proofreading, and preparation of the final version of the manuscript.

All authors reviewed, approved, and agreed to the final manuscript.

Ethics

The authors affirm that this manuscript does not involve human participants, animals, or sensitive data and therefore does not require ethical approval. The authors declare that there are no ethical concerns associated with the publication of this work.

References

Ahsan, R., Shahzadi, I., Najeeb, F., & Omer, H. (2024). Brain tumor detection and segmentation using deep learning. *Magnetic Resonance Materials in Physics, Biology and Medicine*, *38*(1), 13–22. https://doi.org/10.1007/s10334-024-01203-5

Ali, A. A., Hammad, M. T., & Hassan, H. S. (2025). A Co-Evolutionary Genetic Algorithm Approach to Optimizing Deep Learning for Brain Tumor Classification. *IEEE Access*, *13*, 21229–21248. https://doi.org/10.1109/access.2025.3535844

Alwadee, E. J., Sun, X., Qin, Y., & Langbein, F. C. (2025). LATUP-Net: A lightweight 3D attention U-Net with parallel convolutions for brain tumor segmentation. *Computers in Biology and Medicine*, *184*, 109353. https://doi.org/10.1016/j.compbiomed.2024.109353

Amin, M., Nahar, K. M. O., Gharaibeh, H., Nasayreh, A., Alsalmanc, N., Alomar, A., Malkawi, M., Alqasem, N., Smerat, A., Zitar, R. A., Nusier, S., Ezugwu, A. E., & Abualigah, L. (2025). DieT Transformer model with PCA-ADE integration for advanced multi-class brain tumor classification. *Intelligence-Based Medicine*, *11*, 100192. https://doi.org/10.1016/j.ibmed.2024.100192

Amoury, S. E., Smili, Y., & Fakhri, Y. (2025). Design of an Optimal Convolutional Neural Network Architecture for MRI Brain Tumor Classification by Exploiting Particle Swarm Optimization. *Journal of Imaging*, *11*(2), 31. https://doi.org/10.3390/jimaging11020031

Asiri, A. A., Soomro, T. A., Shah, A. A., Pogrebna, G., Irfan, M., & Alqahtani, S. (2024). Optimized Brain Tumor Detection: A Dual-Module Approach for MRI Image Enhancement and Tumor Classification. *IEEE Access*, *12*, 42868–42887. https://doi.org/10.1109/access.2024.3379136

Başarslan, M. S. (2025). a novel classification model for brain tumor classification: multi-CNN and multi-BiLSTM. *The Journal of Supercomputing*, *81*(3), 502. https://doi.org/10.1007/s11227-025-06964-x

BRATS. (2020). Brain Tumor Segmentation (BraTS 2020). *Kaggle / The Cancer Imaging Archive (TCIA) / MICCAI BraTS Challenge*.

Chaoyang, Z., Shibao, S., Wenmao, H., & Pengcheng, Z. (2024). FDR-TransUNet: A novel encoder-decoder architecture with vision transformer for improved medical image segmentation. *Computers in Biology and Medicine*, *169*, 107858. https://doi.org/10.1016/j.compbiomed.2023.107858

Dutta, T. K., Nayak, D. R., & Zhang, Y.-D. (2024). ARM-Net: Attention-guided residual multiscale CNN for multiclass brain tumor classification using MR images. *Biomedical Signal Processing and Control*, *87*, 105421. https://doi.org/10.1016/j.bspc.2023.105421

Figshare. (2017). Figshare Brain Tumor Dataset (Brain Tumor Dataset). *Kaggle*.

Geetha, M., Srinadh, V., Janet, J., & Sumathi, S. (2024). Hybrid Archimedes Sine Cosine optimization enabled Deep Learning for multilevel brain tumor classification using MRI images. *Biomedical Signal Processing and Control*, *87*, 105419. https://doi.org/10.1016/j.bspc.2023.105419

Hosny, K. M., Mohammed, M. A., Salama, R. A., & Elshewey, A. M. (2025). Explainable ensemble deep learning-based model for brain tumor detection and classification. *Neural Computing and Applications*, *37*(3), 1289–1306. https://doi.org/10.1007/s00521-024-10401-0

Huang, Z., Duan, J., Xie, Y., & Liu, Y. (2025). UDNet: Unified Deep Network based on Transformer and Multi-stage Fusion for brain tumor classification from undersampled MRI. *Neurocomputing*, *619*, 129109. https://doi.org/10.1016/j.neucom.2024.129109

Islam, Md. M., Barua, P., Rahman, M., Ahammed, T., Akter, L., & Uddin, J. (2023). Transfer learning architectures with fine-tuning for brain tumor classification using magnetic resonance imaging. *Healthcare Analytics*, *4*, 100270. https://doi.org/10.1016/j.health.2023.100270

Kanchanamala, P., Kuppusamy, V., & Ganesan, G. (2025). QDCNN-DMN: A hybrid deep learning approach for brain tumor classification using MRI images. *Biomedical Signal Processing and Control*, *101*, 107199. https://doi.org/10.1016/j.bspc.2024.107199

Khan, M. A., Khan, A., Alhaisoni, M., Alqahtani, A., Alsubai, S., Alharbi, M., Malik, N. A., & Damaševičius, R. (2023). Multimodal brain tumor detection and classification using deep saliency map and improved dragonfly optimization algorithm. *International Journal of Imaging Systems and Technology*, *33*(2), 572–587. https://doi.org/10.1002/ima.22831

Khan, S. U. R., Zhao, M., & Li, Y. (2025). Detection of MRI brain tumor using residual skip block based modified MobileNet model. *Cluster Computing*, *28*(4), 248. https://doi.org/10.1007/s10586-024-04940-3

Kurdi, S. Z., Ali, M. H., Jaber, M. M., Saba, T., Rehman, A., & Damaševičius, R. (2023). Brain Tumor Classification Using Meta-Heuristic Optimized Convolutional Neural Networks. *Journal of Personalized Medicine*, *13*(2), 181. https://doi.org/10.3390/jpm13020181

Kusuma, P. V., & Reddy, S. C. M. (2025). Brain tumor segmentation and classification using MRI: Modified segnet model and hybrid deep learning architecture with improved texture features. *Computational Biology and Chemistry*, *117*, 108381. https://doi.org/10.1016/j.compbiolchem.2025.108381

Masoud, N. (2021). Brain Tumor MRI Dataset. *Kaggle*. https://www.kaggle.com/datasets/masoudnickparvar/brain-tumor-mri-dataset

Nancy, A. M., & Maheswari, R. (2024). Brain tumor segmentation and classification using transfer learning based CNN model with model agnostic concept interpretation. *Multimedia Tools and Applications*, *84*(5), 2509–2538. https://doi.org/10.1007/s11042-024-20353-1

Nassar, S. E., Yasser, I., Amer, H. M., & Mohamed, M. A. (2024). A robust MRI-based brain tumor classification via a hybrid deep learning technique. *The Journal of Supercomputing*, *80*(2), 2403–2427. https://doi.org/10.1007/s11227-023-05549-w

Popat, M., & Patel, S. (2026). Cascaded MNetV3UNet: A Lightweight Two-Stage Architecture for High-Precision Brain Tumor Segmentation in MRI. *Journal of Computer Science*, *22*(2), 589–604. https://doi.org/10.3844/jcssp.2026.589.604

Pourmahboubi, A., Saeed, N. A., & Tabrizchi, H. (2025). A brain tumor segmentation enhancement in MRI images using U-Net and transfer learning. *BMC Medical Imaging*, *25*(1), 307. https://doi.org/10.1186/s12880-025-01837-4

Sachdeva, J., Sharma, D., & Ahuja, C. K. (2024). Comparative Analysis of Different Deep Convolutional Neural Network Architectures for Classification of Brain Tumor on Magnetic Resonance Images. *Archives of Computational Methods in Engineering*, *31*(4), 1959–1978. https://doi.org/10.1007/s11831-023-10041-y

Selvan, P. S., Addula, S. R., Singh, C. E., Narayanaperumal, M., Marriwala, N. K., & Appathurai, A. (2025). Deep Learning-Enabled Fetal Health Classification Through Sensor-Fused IoT Environment. *Mobile Radio Communications and 5G Networks*, *1328*, 157–169. https://doi.org/10.1007/978-981-96-4226-7_13

Shamshad, N., Sarwr, D., Almogren, A., Saleem, K., Munawar, A., Rehman, A. U., & Bharany, S. (2024). Enhancing Brain Tumor Classification by a Comprehensive Study on Transfer Learning Techniques and Model Efficiency Using MRI Datasets. *IEEE Access*, *12*, 100407–100418. https://doi.org/10.1109/access.2024.3430109

Shreeharsha, J. (2024). Brain Tumor Segmentation and Classification Using Binomial Thresholding-Based Bidirectional-Long-Short Term Memory. *International Journal of Intelligent Engineering and Systems*, *17*(3), 149–158. https://doi.org/10.22266/ijies2024.0630.13

Sobha, X. P., Kumar, S. P., & Govindarajan, R. (2024). Enhanced Postoperative Brain MRI Segmentation with Automated Skull Removal and Resection Cavity Analysis. *Journal of Computer Science*, *20*(5), 585–593. https://doi.org/10.3844/jcssp.2024.585.593

Zhu, Z., He, X., Qi, G., Li, Y., Cong, B., & Liu, Y. (2023). Brain tumor segmentation based on the fusion of deep semantics and edge information in multimodal MRI. *Information Fusion*, *91*, 376–387. https://doi.org/10.1016/j.inffus.2022.10.022

Zhu, Z., Wang, Z., Qi, G., Mazur, N., Yang, P., & Liu, Y. (2024). Brain tumor segmentation in MRI with multi-modality spatial information enhancement and boundary shape correction. *Pattern Recognition*, *153*, 110553. https://doi.org/10.1016/j.patcog.2024.110553